

The influence of Madden–Julian Oscillation in the genesis of North Indian Ocean tropical cyclones

K. S. Krishnamohan · K. Mohanakumar · P. V. Joseph

Received: 12 August 2011 / Accepted: 26 December 2011 / Published online: 12 January 2012
© Springer-Verlag 2012

Abstract Cyclonic storms having maximum winds of 34 knots and above that had genesis in north Indian Ocean have been studied with respect to the eastward passage of Madden–Julian Oscillation (MJO). In the three decades (1979–2008), there were a total of 118 cyclones reported in which 96 formed in the region chosen (0–15°N, 60°E–100°E) for the study. Although the percentage of MJO days inducing cyclogenesis is small, it is found that tropical cyclone genesis preferentially occurred during the convective phase of MJO. This accounted for 44 cyclones of the total 54 cyclones (i.e., 81.5%) formed under MJO amplitude 1 and above. The study has shown that, when the enhanced convection of MJO is over the maritime continent and the adjoining eastern Indian Ocean, it creates the highest favorable environment for cyclogenesis in the Bay of Bengal. During this phase, westerlies at 850 hPa are strong in the equatorial region south of Bay of Bengal creating strong cyclonic vorticity in the lower troposphere along with the low vertical wind shear.

1 Introduction

The relationship between Madden–Julian Oscillation (MJO) and the genesis of the tropical cyclones in the north Indian

Ocean (NIO) has been studied. Convection associated with MJO originates over the equatorial western Indian Ocean, propagates eastward, and then enters the Pacific Ocean crossing the maritime continent. This eastward propagating tropical disturbance with period in the range of 40 to 50 days was first identified by Madden and Julian (1971). Further studies showed that MJO has a broadband spectral period ranging from 30 to 60 days and has a global wave number one structure with a spatial wavelength of roughly 12,000–20,000 km (Nakazawa 1988). This oscillation is associated with eastward-moving convection with an enhanced convective phase followed by a non-convective (suppressed convection) phase at any one location. The low-level wind fields associated with MJO are characterized by fluctuations between easterly and westerly phases and can be observed in several other parameters such as surface pressure, upper tropospheric wind, and proxies for deep convection such as outgoing long-wave radiation (OLR).

Gray (1979) found that the global tropical cyclone formation can be grouped into temporal clusters with an active period of cyclogenesis of a few weeks followed by a few weeks of relatively less cyclogenesis. The relation between MJO and tropical cyclones was analyzed by Nakazawa (1986) for the year 1979 who found that the genesis and growth of tropical cyclones occur globally during the active phase of intraseasonal variations associated with the 30 to 60 day oscillations in OLR. Liebmann et al. (1994) studied the relationship between tropical cyclones of the western Pacific and Indian Ocean with MJO and found that the absolute number of storms and typhoons are enhanced during the convective phase of the MJO compared with the non-convective phase. They reported that there exist more storms and typhoons because of more depressions in the convective phase. Later studies found significant relation between tropical cyclones and MJO over the global ocean

K. S. Krishnamohan (✉) · K. Mohanakumar · P. V. Joseph
Department of Atmospheric Sciences,
Cochin University of Science and Technology,
Fine Arts Avenue,
Cochin 682016 Kerala, India
e-mail: krishmet@gmail.com

K. Mohanakumar
e-mail: kmkcsat@gmail.com

P. V. Joseph
e-mail: joporathur@gmail.com

basins, such as Maloney and Hartmann (2000a) for Gulf of Mexico and for eastern North Pacific (Maloney and Hartmann 2000b); Hall et al. (2001) for the Australian region; Maloney and Hartmann (2001) and Hartmann and Maloney (2001) for north Pacific Ocean; Bessafi and Wheeler (2006) for south Indian Ocean; Kim et al. (2008) for the western north Pacific; Klotzbach (2010) for the Atlantic Ocean; and Kikuchi and Wang (2010) for NIO. Kikuchi and Wang (2010) have studied cyclogenesis in NIO associated with both the northward-moving boreal summer intra-seasonal oscillation and the eastward-moving MJO.

The relation between MJO and tropical cyclones can be attributed to the deep convection in the convective phase and the associated strengthening of equatorial lower tropospheric westerly wind toward the west of the area of convection (Rui and Wang, 1990). Such a situation leads to an increase in cyclonic vorticity in the atmospheric boundary layer of the low latitude regions north and south of the equator. MJO is also characterized by enhanced upper level divergence associated with the convective phase. For the genesis of tropical cyclones, certain large-scale tropical features were identified by Gray (1968), such as sufficient thermal energy in the top layer of the ocean, enhanced mid-tropospheric relative humidity, conditional instability to trigger deep moist convection, increased lower tropospheric relative vorticity, weak vertical shear of the horizontal winds, and location at least 5° latitude away from the equator.

Liebmann et al. (1994) observed that the cyclones preferentially occur during the convective phase of MJO and cluster around the low-level cyclonic vorticity and upper-level divergence anomalies that appear poleward and westward of the large-scale convective anomaly along the equator. Later studies have shown the importance of eddy kinetic energy associated with the convective phase of MJO in the formation of cyclones. Maloney and Hartmann (2001) noticed that, when 850-hPa wind anomalies of MJO are westerly, small-scale slow-moving eddies grow through barotropic eddy kinetic energy conversion from the mean flow, and these growing eddies, together with strong surface convergence, 850 hPa cyclonic wind shear (vorticity), and high mean sea surface temperatures create a favorable environment for tropical cyclone formation. Leroy and Wheeler (2008) developed a statistical scheme to predict the tropical cyclone activity in the southern hemisphere using five predictors in which two represents the eastward propagation of the MJO, two represents the leading patterns of interannual sea surface temperature variability in the Indo-Pacific Oceans and one represent the climatological seasonal cycle of tropical cyclone activity in each zone. They found that inclusion of indices of the MJO as predictors leads to increased skill out to about 3 weeks.

Roundy (2008) discussed in detail the interaction of convectively coupled Kelvin wave with MJO in NIO basin and has shown that the MJO phase modulates the intensity of moist deep convection associated with the Kelvin waves. The role of convectively coupled waves like MJO, convectively coupled equatorial Rossby, Kelvin, and mixed Rossby–gravity waves in the modulation of south Indian Ocean tropical cyclones were analyzed by Bessafi and Wheeler (2006) who studied the dynamical controls of these waves on tropical cyclone through wave-induced perturbations to the dynamical fields of low-level vorticity, vertical wind shear (VWS), and deep convection. They have shown that large-scale atmospheric variability caused by MJO and equatorial Rossby waves is important for the modulation of tropical cyclones in south Indian Ocean and can be used for prediction purposes extending up to few weeks.

The frequency of tropical cyclones in the NIO basin has a bimodal structure with cyclones occurring from September to December with a primary maximum in November and

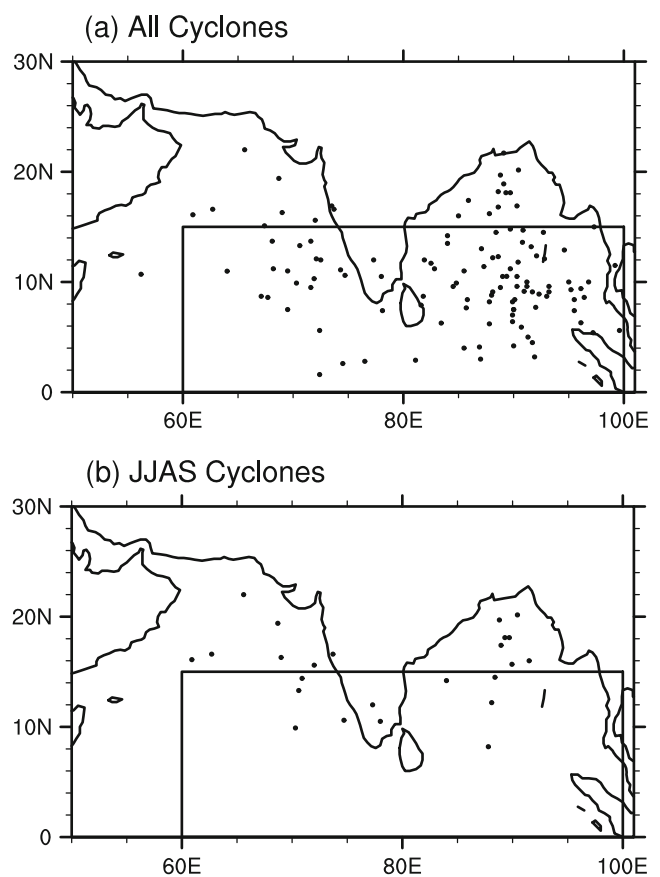


Fig. 1 Tropical cyclone genesis location (dots) for the three decades from 1979 to 2008. The rectangular area marked in the figure shows the region selected for the study ($0\text{--}15^\circ\text{N}$, $60^\circ\text{E}\text{--}100^\circ\text{E}$). **a** Total 118 cyclones formed during 1979 to 2008; **b** Cyclones which formed from June to September

Table 1 Month-wise distribution of the cyclones and those formed in the study region

Total	Jan	Feb	Mar	Apr	May	Jun	Jul	Aug	Sep	Oct	Nov	Dec
118	4	0	3	5	21	10	1	1	7	21	34	11
96	4	0	2	5	17	6	0	0	3	16	32	11

from April to mid June with a secondary maximum in May (McBride 1995). A detailed climatology of the tropical cyclones over NIO is available in the storm atlas of India Meteorological Department (IMD Atlas 1979). The cyclones having their genesis in the area bounded by latitudes 0° to 15°N and longitudes 60°E to 100°E has been studied as outside this area very few cyclones have their genesis in the pre-monsoon and post-monsoon seasons. In the Indian summer monsoon season (June to September), monsoon depressions (cyclonic systems weaker than tropical cyclones) are formed, and their genesis area is north of the area chosen for the study. During the monsoon season, very few of the cyclonic systems formed develop into cyclone intensity due to the prevailing high VWS in the environment, with monsoon low-level jet stream in the lower troposphere and the tropical easterly jet stream in the upper troposphere.

2 Data and methodology

The real-time multivariate MJO index (RMM) developed by Wheeler and Hendon (2004), available at <http://cawcr.gov.au/staff/mwheeler/maproom/RMM/> is used in this study. This index is developed based on the first two empirical orthogonal functions (EOF) of the combined fields of equatorially averaged 850 hPa zonal wind, 200 hPa zonal wind, and OLR. The two leading principal components corresponding to the two EOFs, known as real-time multivariate MJO series 1 and 2 (RMM1 and RMM2, respectively) is used to calculate the phase and amplitude of eastward MJO propagation. The amplitude and the phase of MJO for each day in the entire time period are provided in the dataset.

OLR data from National Oceanic and Atmospheric Administration (NOAA) polar orbiting satellites (Liebmann and Smith 1996) available from 1974 onwards are used in the study. Global reanalysis data from the National Centers for Environmental Prediction/National Center for Atmospheric Research (NCEP/NCAR) (Kalnay and Coauthors 1996) were used for winds at 200 and 850 hPa levels. Both these datasets are daily means and available on $2.5^{\circ}\times 2.5^{\circ}$ latitude–longitude grid.

Tropical cyclone data from the International best Track Archive for Climate Stewardship (IBTrACS) (Knapp et al. 2010) from 1979 to 2008 is used in the study. For the Indian Ocean basin, this data set is derived from various sources

like Joint Typhoon Warning Center (JTWC) (Pearl Harbor, Hawaii) and the Regional Specialized Meteorological Center (RSMC) New Delhi. The data discrepancy between different sources used in IBTrACS dataset is discussed in Knapp and Kruk (2010).

The MJO days can be clustered into eight phases (P1, P2, P3... P8, hereafter) depending on the phase-angle variations in the phase space created by the RMM1 and RMM2 indices (Wheeler and Hendon 2004). Each phase represents the geographical location of the enhanced convection of the MJO with respect to the phase space. On this, the phases P1, P2, P3, and P4 represent the convective phase of MJO where the equatorial Indian Ocean is dominated by convection. Similarly, the phases P5, P6, P7, and P8 represent the period when convection is suppressed in the equatorial Indian Ocean. The genesis dates of cyclones are clustered into these eight groups based on the MJO phase in which a cyclone genesis date resides. The genesis date of a cyclone is defined as the first day of the cyclone reported in the IBTrACS dataset.

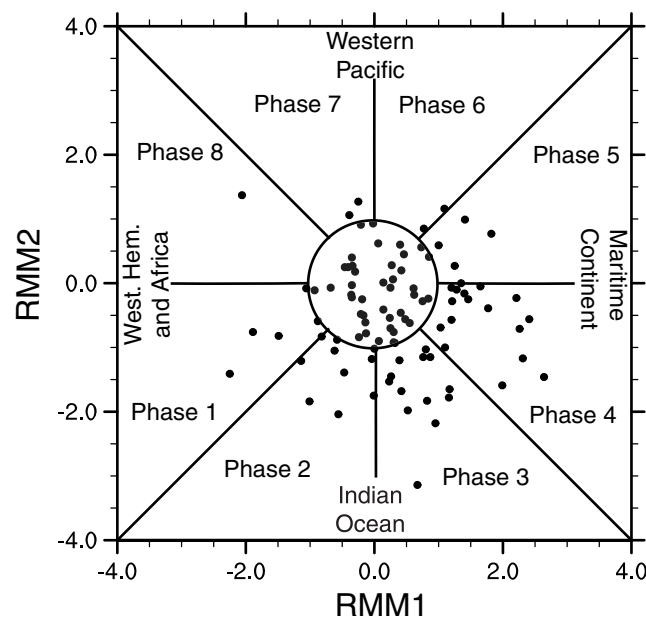


Fig. 2 Phase amplitude diagram constructed with the principal components RMM1 and RMM2 of MJO from 1979 to 2008. The black dots represent the cyclogenesis days. Eight categories are defined according to the phase angle in which a day resides. The circle in the center with amplitude 1 represents days with weak MJO activity

Table 2 Summary of the distribution of tropical cyclone genesis days in the different categories of MJO for the various amplitudes taken

MJO amplitude	No. of cyclones	P1	P2	P3	P4	P5	P6	P7	P8
0.5	83	7	15	22	20	8	4	5	2
1	54	5	10	13	16	5	2	2	1
1.5	27	3	4	8	8	2	1	0	1

Following Hall et al. (2001), a statistical analysis of the significance of the number of tropical cyclone in each MJO category is done. Here, a Z statistic is calculated for the eight phases of MJO, taking the null hypothesis that cyclones are equally distributed in all the phases. The statistic is given as

$$Z = \frac{p - p_0}{\sqrt{p_0(1 - \frac{p_0}{N})}} \tag{1}$$

Where p and p_0 are expected and observed proportion of cyclogenesis days within a particular MJO category, respectively, and N is the number of days in the category. It was tested at the 95%, 98%, and 99% levels, using a two-tailed test, with critical values of $Z = \pm 1.96, \pm 2.326, \text{ and } \pm 2.576$, respectively.

3 Results

3.1 Genesis and distribution of cyclones

From IBTrACS cyclone data, cyclonic systems with maximum sustained wind speed of 34 knots or above, which is the criteria used by India Meteorological Department for NIO cyclone, are used in the study. Using this criteria, 118 cyclones were identified which satisfy the intensity criteria for NIO basin from 1979 to 2008. Out of the 118 cyclones selected, 96 cyclones had their genesis in the study region. Figure 1 gives the distribution of the genesis points of

cyclones in which the area inside the box (0–15°N and 60°E–100°E) represents the area of cyclogenesis selected for the study. Figure 1a represents the total 118 cyclones formed, and Fig. 1b gives the cyclones which originated during June to September (JJAS). It can be seen that majority of the JJAS cyclones had their genesis outside the study area. The month-wise distribution of the total 118 cyclones selected and the 96 cyclones having their genesis located in the study region are given in Table 1. It may be seen that, during the monsoon season (June to September), very few cyclones have formed. Similarly, there are few cyclones in February and March. Cyclone prone months are April and May and October to December which account for the majority of cyclogenesis in the area.

A phase space diagram is created using the RMM1 and RMM2 indices to represent the different phases of MJO. The phase space diagram along with the distribution of cyclones is given by Fig. 2. In Fig. 2, the circle in the center of phase space with radius 1 represents days with MJO amplitude 1 and less. The black dots represent the date of cyclogenesis. Any day falling inside this circle is considered as a weak MJO day. From the phase-space diagram, it can be seen that cyclogenesis dates are clustered on the convective phase of MJO (P1 to P4). Although cyclogenesis occurred in the suppressed convection phases of MJO, majority of the days are under MJO amplitude 1.

The distributions of cyclones in different MJO categories were studied by setting different amplitudes of MJO. The MJO amplitudes, total number of cyclones formed under each amplitude and distribution of cyclones in each MJO

Table 3 Month-wise distribution of cyclones in each phase of MJO

Month	Jan	Feb	Mar	Apr	May	Jun	Jul	Aug	Sep	Oct	Nov	Dec
Phase												
1	–	–	–	1	2	–	–	–	–	–	2	–
2	–	–	1	–	2	1	–	–	1	1	4	–
3	2	–	–	–	6	2	–	–	–	–	1	2
4	–	–	–	1	3	2	–	–	–	–	9	1
5	–	–	–	–	–	–	–	–	–	–	4	1
6	1	–	–	–	1	–	–	–	–	–	–	–
7	–	–	–	–	–	–	–	–	–	1	1	–
8	–	–	–	–	1	–	–	–	–	–	–	–
Total	3	0	1	2	15	5	0	0	1	2	21	4

phase are given in Table 2. The first column in Table 2 represents the MJO amplitude, and the second column gives the total number of cyclones for the corresponding phase. Columns from 3 to 10 give the distribution of genesis days

within the eight phases of MJO. The MJO amplitude 0.5 covers approximately 89% of the total days which include the majority of the cyclogenesis and accounts for 83 cyclones out of the total 96 cyclones formed in the study

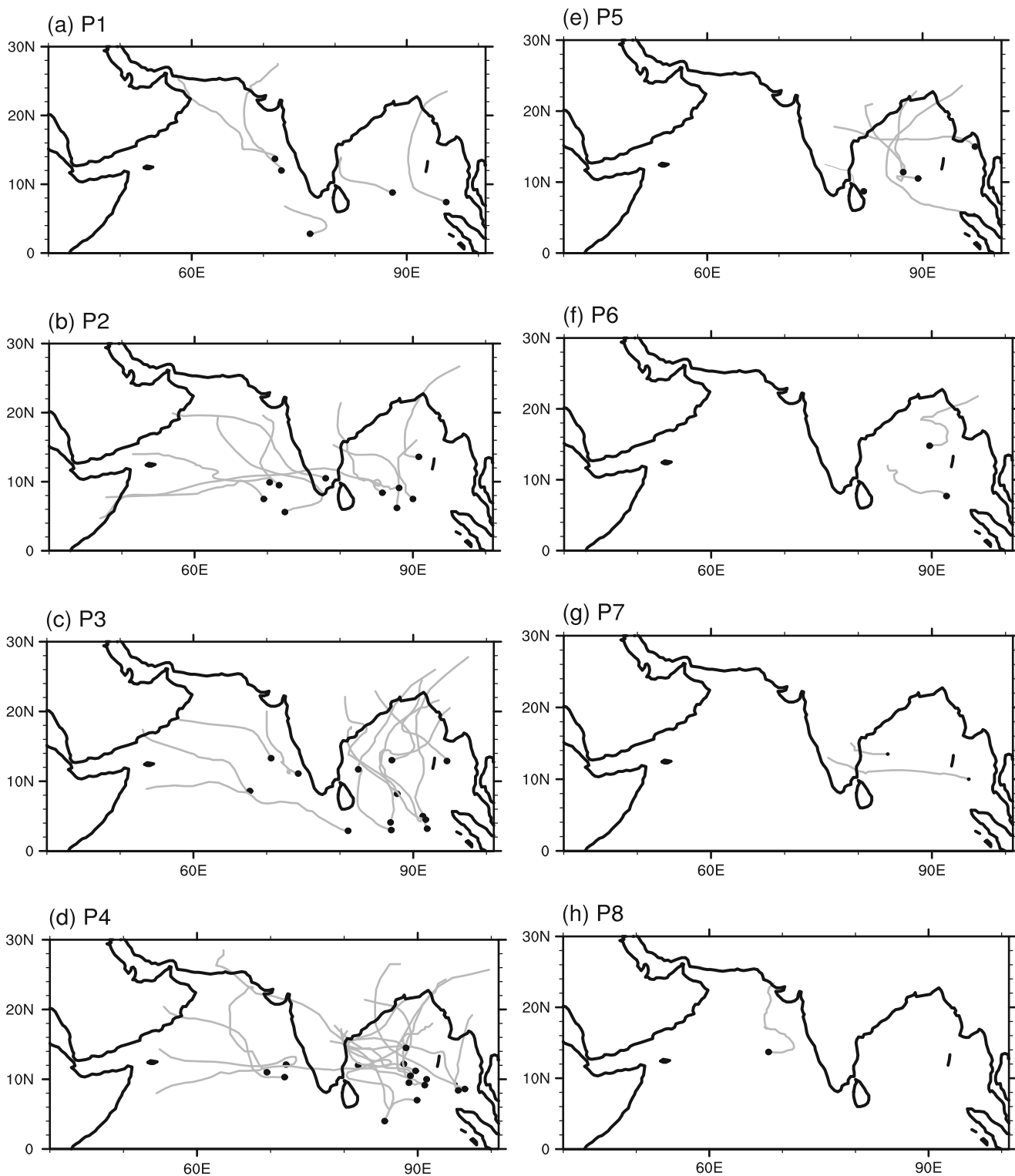


Fig. 3 Tropical cyclone genesis location (*dots*) and tracks (*lines*) for different MJO phases

area. Out of this 83 cyclones, seven (8.4%) formed in P1, 15 (18%) in P2, 22 (26.5%) in P3, and 20 (24.1%) in P4. For MJO amplitude 1, which includes approximately 61% of the total days, 54 cyclones are formed. Out of this 54 cyclones, five (9.3%) formed in P1, 10 (18.5%) in P2, 13 (24.1%) in the P3, and 16 (29.3%) in the P4. Convective phase of MJO (P1, P2, P3, and P4) accounts for 44 (81.5%) of cyclones formed under MJO amplitude 1. Using the statistic defined earlier the number of cyclones, phases P3 and P4 are found to be significantly high at 98% significance level. For MJO amplitude of 1.5 which includes 33.4% of the total days, 27 cyclones formed. Here, 22 out of 27 cyclones originated in the convective phase of MJO. In all cases, it is seen that the number of cyclogenesis days are more in the convective phases compared with the suppressed convection phases.

The month-wise distribution of the tropical cyclone genesis in each phase is given in Table 3. As seen from Table 3, the monthly distributions of cyclones within the MJO phases are also showing the bimodal structure similar to the general NIO cyclone variability. As we can see, the bimodal peak has its largest amplitude during November to December which accounts for 25 cyclones followed by May–June accounting 20 cyclones. For P3, more cyclones formed in May–June period; but for P4, majority of cyclones are formed in November–December period. Thus, we have two distinct periods (May–June and November–December) of cyclogenesis for each MJO phase which is used to analyze the prevailing synoptic conditions for the phases.

The spatial distribution of cyclogenesis with the genesis points and tracks of tropical cyclones in each MJO phases are shown in Fig. 3. Here, only the days with MJO

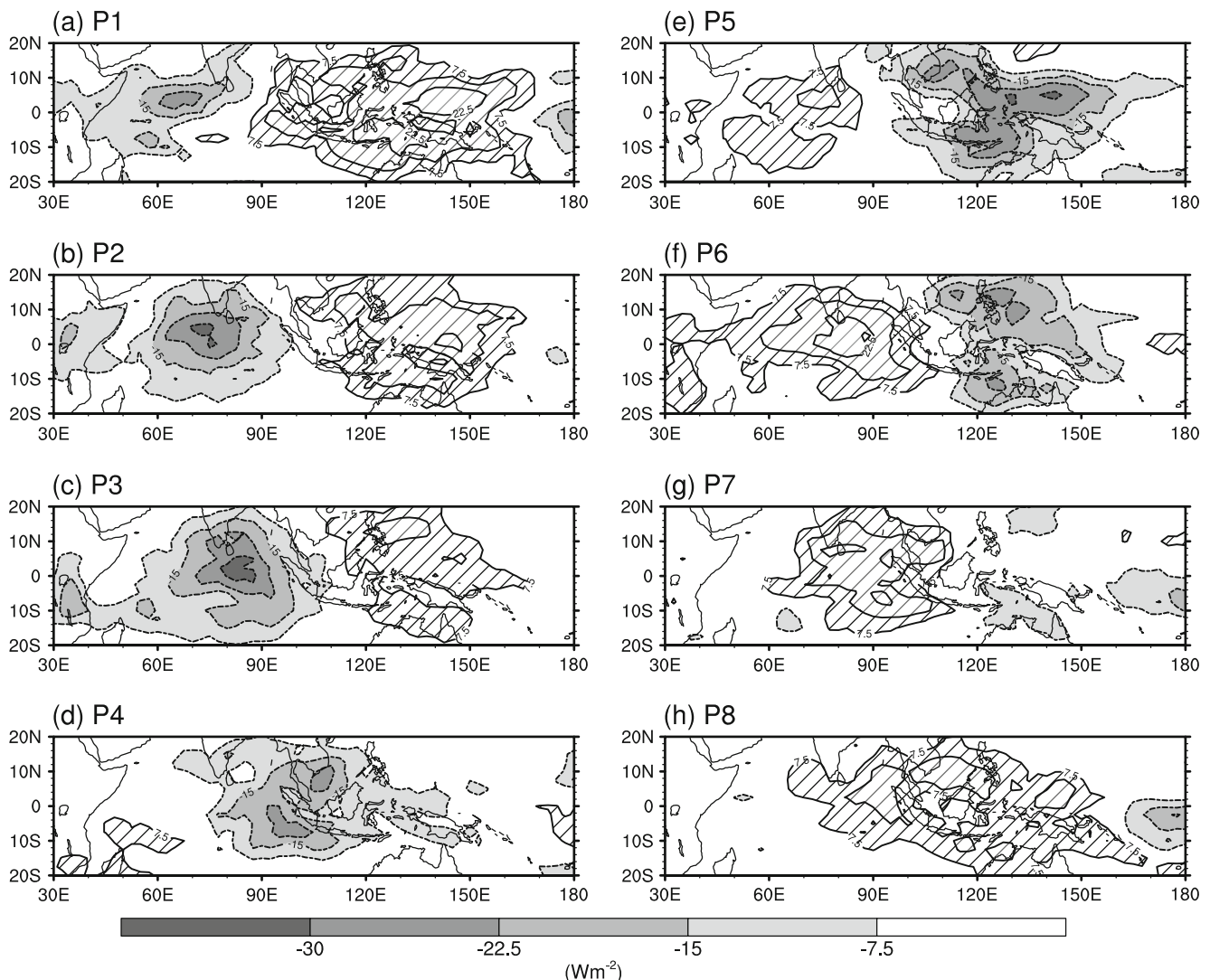


Fig. 4 OLR anomaly composites of November–December associated with MJO phases 1 to 8. The negative contours are shaded and the positive anomaly contours are hatched. The contour interval is 7.5 Wm^{-2}

amplitude 1 or above is considered. Figure 3a–d represents the convective phases of MJO, and Fig. 3e–h represents the suppressed convection phase. For phases P1 and P2, although the number of tropical cyclones is less, they are distributed almost equally in the Arabian Sea (AS) and Bay of Bengal (BOB). But for phases P4 and P5, more cyclones are formed in the BOB comparing with AS. For phases P5 to P8, the cyclogenesis occurred mainly in the BOB. The spatial distributions of cyclones are found to be highly influenced by the synoptic conditions associated with the MJO categories. A detailed discussion about the synoptic conditions leading to cyclogenesis and distribution during the phases are given in the following section.

3.2 Synoptic conditions

Synoptic conditions associated with each phase of MJO are studied by compositing the different parameters related with

cyclogenesis such as OLR, sea surface temperature (SST), 850 hPa wind flow, 850 hPa vorticity, and the VWS between 200 and 850 hPa. SST of the study region has remained higher than 28⁰ C in all the MJO phases during November–December. In May–June, SSTs are still higher. Our study has shown that SST is not an important factor for cyclogenesis in the study region with respect to the phases of MJO. However, the large-scale circulation patterns and associated changes in environmental parameters such as 850 hPa relative vorticity and VWS are important in modulating the tropical cyclone activity over the ocean basins (Chand and Walsh 2009 ; Belanger et al. 2010). Composites of these fields are analyzed in the study to bring out the favorable conditions which led to cyclogenesis. For each phase, the days having MJO amplitude 1 or above are composited for the months under consideration. The anomalies are calculated from these fields by subtracting the climatological mean of the months from 1979 to 2008.

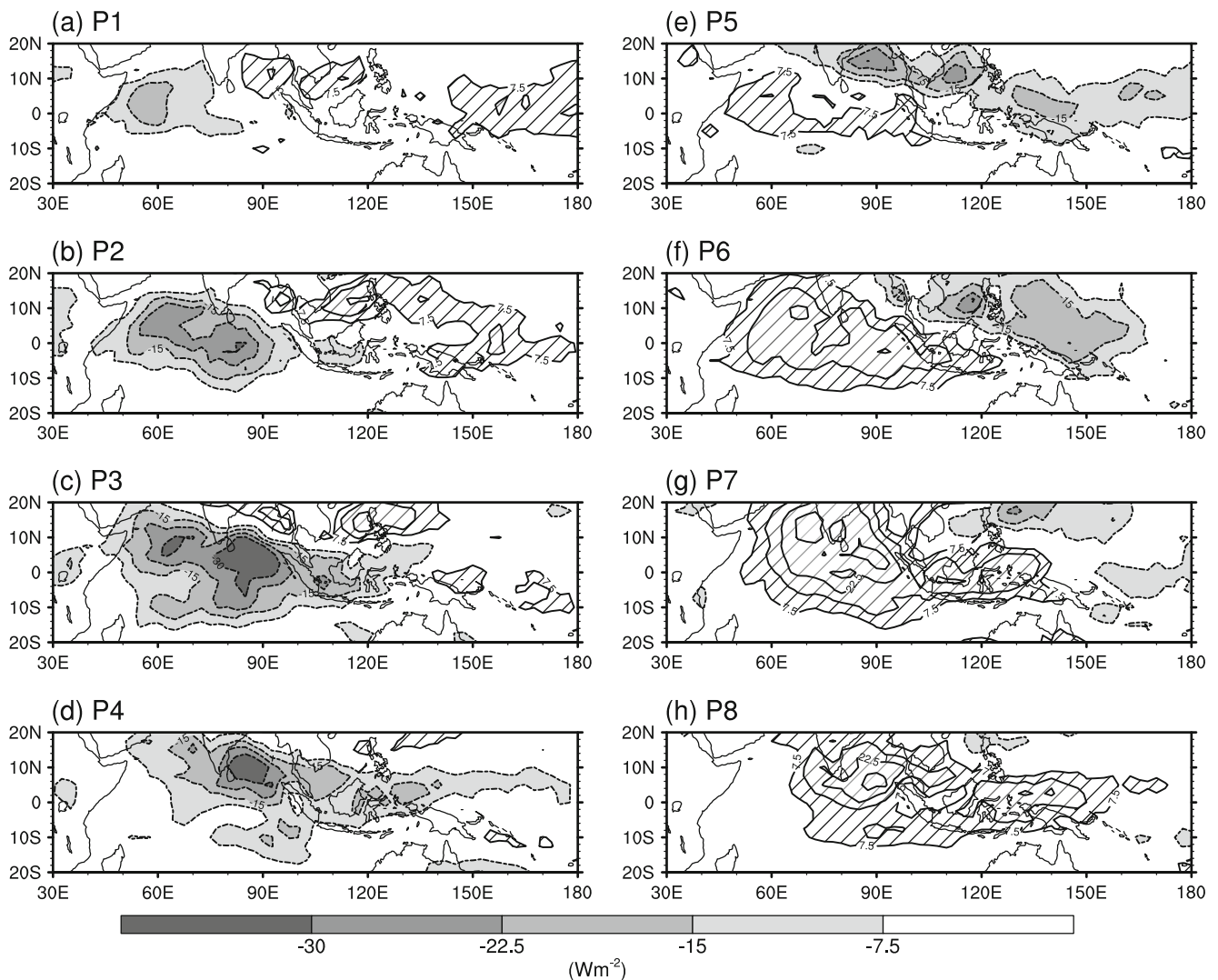


Fig. 5 Same as Fig. 4, but for May–June

The OLR anomaly patterns for November–December are given in Fig. 4. The eight phases of MJO convection are depicted in the figure which shows the temporal varying patterns for the season. It is seen that, during the phases P1 to P4, the area of convection is located over the Indian Ocean. During P1, the convection is in its initial phase with a small patch extends over the Arabian Sea. During P2, the convection has shifted to central Indian Ocean, and from there, it has shifted to eastern Indian Ocean during P3. This convection further extends in P4 covering the entire eastern Indian Ocean and maritime continent. During P5, the convection over maritime continent strengthens, but there is suppressed convection generating over the western Indian Ocean. This suppressed convection follows the same development pattern as in the convective phase of MJO by subsequent development of suppressed convection from P5 to P8. The May–June convection patterns for the same

phases are given in Fig. 5 which are identical with those given in Wheeler and Hendon (2004). Similar to P1 of November–December, here, the first phase (P1) of MJO consists of weak convection over the AS. During P2, this further extends into central Indian Ocean. In P3, convection covers the entire Indian Ocean and reaches up to the maritime continent. This convection moves further eastward during P4 with a slight northward movement with an elongated patch reaching western Pacific and covering the entire Indian Ocean. From P5 to P8, suppression phase of MJO exists over the Indian Ocean with its development patterns similar to the convective phases.

Wind anomaly patterns associated with the MJO convection during November–December is given in Fig. 6. The cyclone genesis points are also given in the figure for each phase as black dots. Only the positive vorticity anomaly (cyclonic vorticity) regions are shown in the diagram as

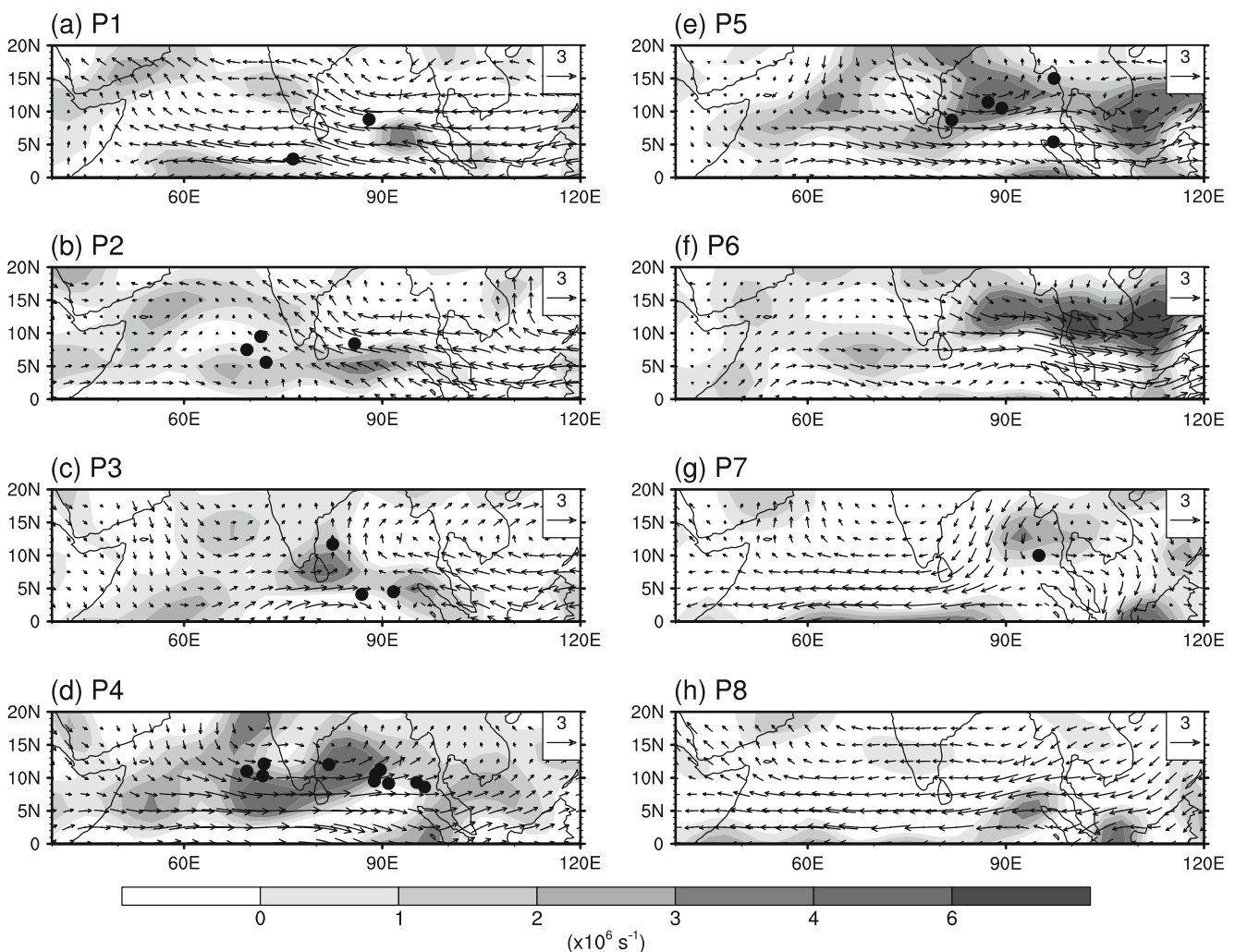


Fig. 6 Composite 850 hPa wind and vorticity anomalies of November–December associated with MJO phases. Wind magnitude and direction is shown by the *arrows*. Reference vector is given in the *upper right corner*.

Contours of cyclonic vorticity are also shown as *shaded*. Vorticity values are scaled by 1×10^{-5} and the contour interval is $1 \times 10^{-5} \text{ s}^{-1}$. The cyclone genesis points are given as *black dots*

shaded regions. It is seen that the cyclones are clustered around the cyclonic vorticity anomaly formed during the passage of MJO convection. In P1, as the convective region is generated over AS, easterly wind anomaly exits over the NIO. Two cyclones had genesis in the equatorial AS and BOB near areas of cyclonic vorticity. As the convection moves eastward in P2, anomalous westerly flow is generated in the NIO especially in AS and the cyclones get formed in the cyclonic vorticity region associated with this. As the MJO convection shifts further eastward during P3, the westerly flow enter the BOB creating a favorable vorticity region for the genesis of cyclones there. The anomalous westerly flow is strengthened further in the entire NIO during P4, which account for ten cyclones formed in its cyclonic vorticity region. As the convection moves to the western Pacific, the westerly wind strengthens over the BOB and five cyclones are formed. Thus, P5 is favorable for cyclogenesis in NIO, particularly the BOB, although the convection is suppressed there. In effect, the phases P1 to P5 favor cyclogenesis in NIO. From

P6 to P8, although vorticity is favorable, the other environmental factors like suppressed convection and VWS (discussed later) inhibit cyclogenesis in NIO.

Composites for May–June are shown in Fig. 7. Similar to November–December, the westerly wind anomalies are generated which move eastwards along with the convection. Westerly wind maximum occurs during the phases P3 and P4 which accounts for the maximum cyclogenesis in NIO. During P3, vorticity maximum exits over the AS and BOB accounting for eight cyclones. In P4, the vorticity maximum region shifts eastwards, and five cyclones are formed in the BOB. During the phase P5, cyclonic vorticity is strong over BOB, but there is no cyclogenesis. In phases P5 to P8, there is little cyclogenesis as both vorticity and VWS (discussed later) are unfavorable along with the suppressed convection existing over NIO.

Figures 8 and 9 represent the VWS composites for November–December and May–June seasons, respectively. During November–December, the VWS is found

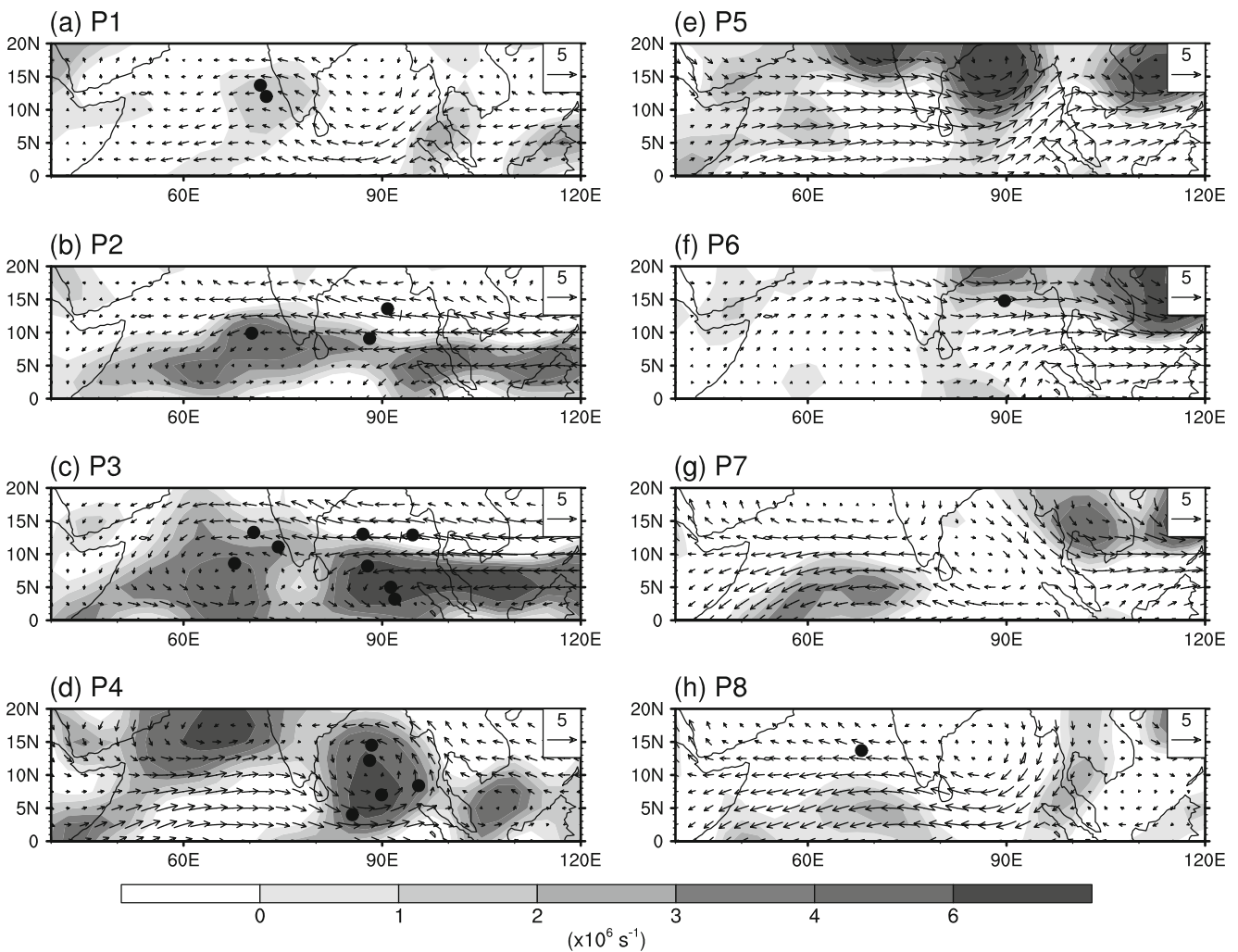


Fig. 7 Same as Fig. 6, but for May–June

to be favorable for the study region in MJO phases P2 to P5, and cyclogenesis occurs with VWS less than 8 ms^{-1} . In the other phases, VWS is more than 8 ms^{-1} , and there is very little cyclogenesis in the study area. Comparing with November–December, the VWS over the study region is higher during May–June. Cyclones have occurred in large numbers during the phases P3 and P4. In these phases, VWS is in the order of 8 to 16 ms^{-1} . Cyclones have occurred with these high shear values in this season, most likely due to the high cyclonic vorticity available at 850 hPa (see Fig. 7).

4 Summary and conclusions

Formation of cyclonic storms over NIO in the area bounded by latitudes 0 and 15°N and longitudes 60°E and 100°E during the period 1979 to 2008 have been studied with respect to the eastward passage of Madden–Julian Oscillation. In this study, MJO intensity with amplitude 1 and above is considered, which includes 61.24% days of the

whole period. There were a total of 118 cyclones in the three decades out of which 96 formed in the study region. The relationship between these cyclones with the different phases of MJO has been studied.

The cyclones are clustered in eight phases of MJO and have been analyzed by selecting different amplitude criteria. The number of the MJO days for each amplitude varies significantly from one to another. However, irrespective of the amplitudes chosen, it is observed that cyclogenesis over NIO basin preferentially occurred during the convective phase of MJO (P1 to P4). By selecting MJO amplitude 1 and above, 81.5% of the cyclones formed was under the convective phase of MJO. Further increasing the amplitude to 1.5 convective phase of MJO dominates by accounting 22 out of the 27 cyclones formed. The study has also shown that P3 and P4 of MJO have the highest favorable environment for cyclogenesis in BOB.

The spatial distribution of the cyclogenesis is seen to be highly associated with the synoptic conditions existing over the NIO during the phases. Phases P1 and P2 are associated

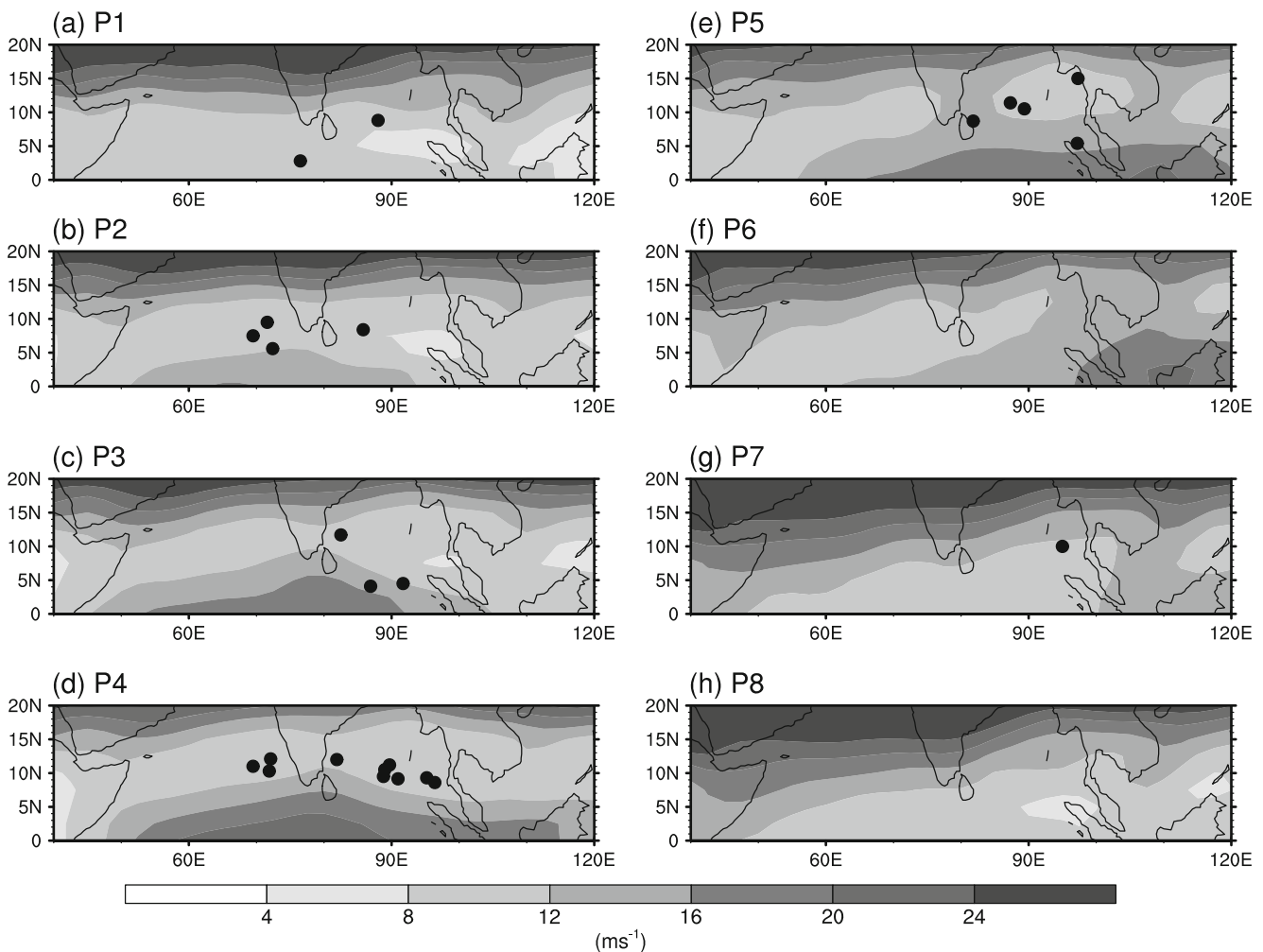


Fig. 8 Composite VWS associated with MJO phases during November–December. The cyclogenesis points are given as *black dots*

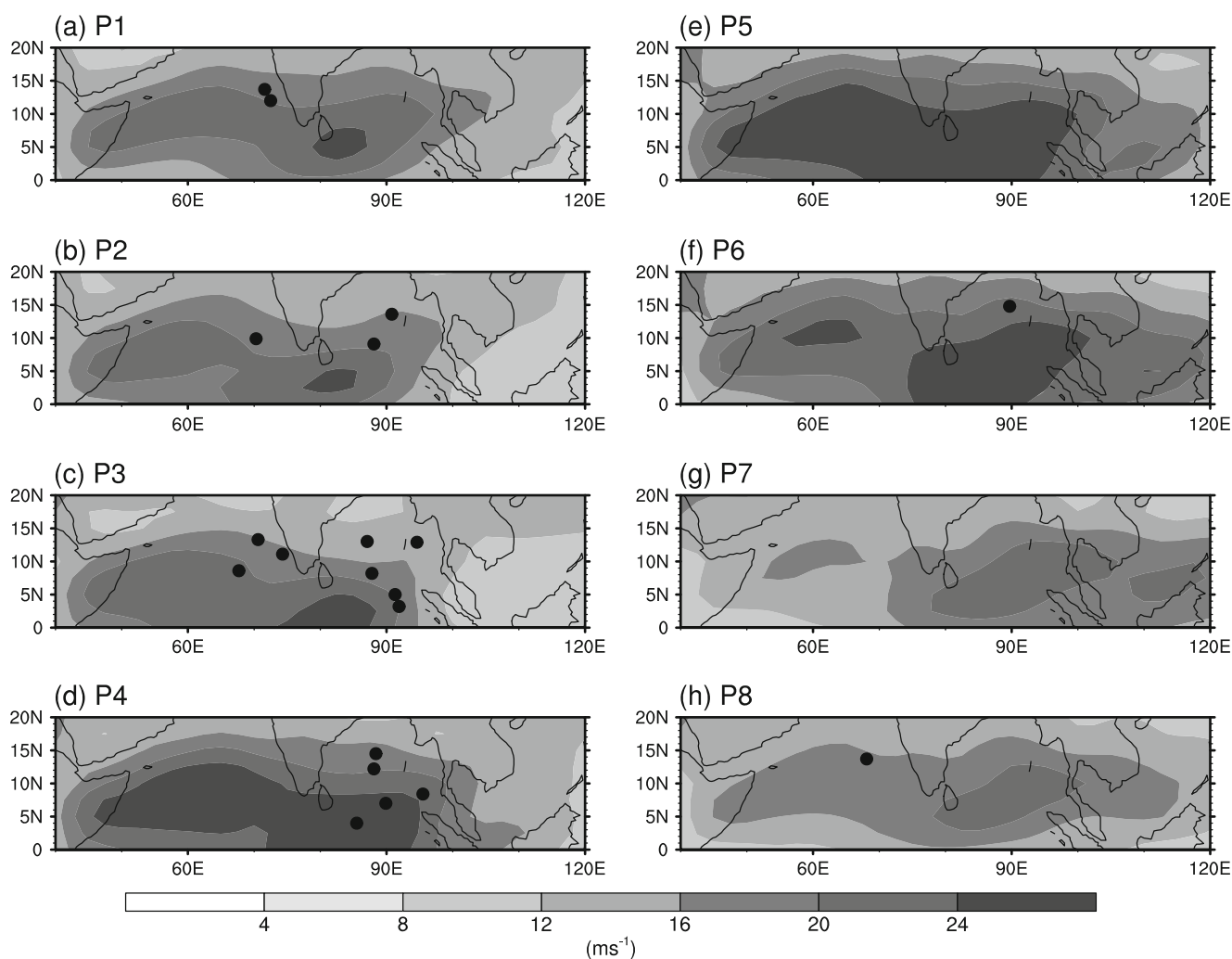


Fig. 9 Same as Fig. 8, but for May–June

with the initial phase of the MJO cycle where active convection occurs over equatorial Indian Ocean. This active convection area will induce strong equatorial westerlies to its west and associated cyclonic vorticity. The cyclogenesis location is seen to be distributed in the AS and BOB almost equally. In the next three phases of the MJO cycle (P3 and P5), the equatorial area of active convection has moved to the BOB and the adjoining western Pacific and the associated westerlies in the lower troposphere cover the whole of equatorial Indian Ocean and is particularly strong over the equatorial areas south of BOB. These phases are thus most favorable for cyclogenesis in the BOB. The cyclogenesis locations are seen to be distributed more in the BOB comparing with AS. In phases P6 to P8, the equatorial convection has moved further east, and the subsiding motion in the NIO leads to suppressed convection and thereby develops unfavorable conditions for cyclogenesis.

The cyclogenesis parameters were composited and analyzed for the different phases of MJO particularly 850 hPa

wind, 850 hPa vorticity. The cyclonic vorticity appearing the north and south of the flow induced by the westerly phases of MJO are significantly influencing the cyclogenesis. The axis of the 850 wind maxima, particularly the zonal component is seen to be shifting from AS to BOB changing the location of cyclogenesis. VWS is found to be favorable during the P3 and P4 phases of November–December and May–June seasons which account for the maximum number of cyclone formation in those phases.

In this study, intensification trends or the direction of movement of tropical cyclones in any category were not examined. Although the convective phase of MJO is found to be favorable for cyclogenesis, further studies are needed for using MJO as an effective predictor of cyclogenesis in NIO.

Acknowledgments The authors would like to acknowledge the facilities provided by Cochin University of Science and Technology, India, to carry out this research. The first author (KKS) is thankful to

Council for Scientific and Industrial Research, India, for providing the fellowship supporting the research.

References

- Atlas IMD (1979) Tracks of storms and depressions in the Bay of Bengal and the Arabian Sea. India Meteorological Department, New Delhi, India
- Belanger JJ, Curry JA, Webster PJ (2010) Predictability of north Atlantic tropical cyclone activity on intraseasonal time scales. *Mon Weather Rev* 138:4362–4374
- Bessafi M, Wheeler MC (2006) Modulation of south Indian Ocean tropical cyclones by the Madden–Julian oscillation and convectively coupled equatorial waves. *Mon Weather Rev* 134:638–656
- Chand SS, Walsh KJE (2009) Tropical cyclone activity in the Fiji region: spatial patterns and relationship to large-scale circulation. *J Clim* 22(14):3877–3893
- Gray WM (1968) Global view of the origin of tropical disturbances and storms. *Mon Weather Rev* 96:669–700
- Gray WM (1979) Hurricanes: their formation, structure, and likely role in the tropical circulation. In: Shaw DB (ed) *Meteorology over the tropical oceans*. Royal Meteorological Society, London, pp 155–218
- Hall JD, Matthews AJ, Karoly J (2001) The modulation of tropical cyclone activity in the Australian region by the Madden–Julian oscillation. *Mon Weather Rev* 129:2970–2982
- Hartmann DL, Maloney ED (2001) The Madden–Julian Oscillation, barotropic dynamics, and north Pacific tropical cyclone formation. Part II: stochastic barotropic modeling. *J Atmos Sci* 58:2559–2570
- Kalnay E, Coauthors (1996) The NCEP/NCAR 40-year reanalysis project. *Bull Am Meteorol Soc* 77:437–471
- Kikuchi K, Wang B (2010) Formation of tropical cyclones in the northern Indian Ocean associated with two types of tropical intraseasonal oscillation modes. *J Meteorol Soc Jpn* 88(3):475–496
- Kim JH, Ho CH, Kim HS, Cui CH, Park SK (2008) Systematic variation of summertime tropical cyclone activity in the western North Pacific in relation to the Madden–Julian oscillation. *J Clim* 15:1171–1191
- Klotzbach PJ (2010) On the Madden-Julian Oscillation–Atlantic hurricane relationship. *J Clim* 23:282–293
- Knapp KR, Kruk MC (2010) Quantifying interagency differences in tropical cyclone best-track wind speed estimates. *Mon Weather Rev* 138(4):1459–1473
- Knapp KR, Michael CK, David HL, Howard JD, Neumann CJ (2010) The International Best Track Archive for Climate Stewardship (IBTrACS): unifying tropical cyclone data. *Bull Am Meteorol Soc* 91:363–376
- Leroy A, Wheeler MC (2008) Statistical prediction of weekly tropical cyclone activity in the Southern Hemisphere. *Mon Weather Rev* 136:3637–3654
- Liebmann B, Smith CA (1996) Description of a complete (interpolated) OLR dataset. *Bull Am Meteorol Soc* 77:1275–1277
- Liebmann B, Hendon HH, Glick JD (1994) The relationship between tropical cyclones of the western Pacific and Indian Oceans and the Madden–Julian oscillation. *J Meteorol Soc Jpn* 72:401–412
- Madden RA, Julian PR (1971) Detection of a 40–50 day oscillation in the zonal wind in the tropical Pacific. *J Atmos Sci* 28:702–708
- Maloney ED, Hartmann DL (2000a) Modulation of eastern North Pacific hurricanes by the Madden–Julian Oscillation. *J Clim* 13:1451–1460
- Maloney ED, Hartmann DL (2000b) Modulation of hurricane activity in the Gulf of Mexico by the Madden–Julian Oscillation. *Science* 287:2002–2004
- Maloney ED, Hartmann DL (2001) The Madden–Julian Oscillation, barotropic dynamics, and North Pacific tropical cyclone formation. Part I: observations. *J Atmos Sci* 58:2545–2558
- McBride JL (1995) Tropical cyclone formation. Global perspective on tropical cyclones, WMO Tech Doc. 693, World Meteorological Organization, 63–105.
- Nakazawa T (1986) Intraseasonal variations of OLR in the tropics during the FGGE year. *J Meteorol Soc Jpn* 64:17–34
- Nakazawa T (1988) Tropical super clusters within intraseasonal variations over the western Pacific. *J Meteorol Soc Jpn* 66:823–839
- Roundy PE (2008) Analysis of convectively coupled Kelvin waves in the Indian Ocean MJO. *J Atmos Sci* 65:1342–1359
- Rui H, Wang B (1990) Development characteristics and dynamic structure of tropical intraseasonal convection anomalies. *J Atmos Sci* 47:357–379
- Wheeler MC, Hendon HH (2004) An all-season real-time multivariate MJO index: development of an index for monitoring and prediction. *Mon Wea Rev* 132:1917–1932